

MEASUREMENTS AND MODELS OF THE ATTENUATION OF AIRCRAFT ENGINE TESTING NOISE

Keith Attenborough
Oleksander Zaporozhets

School of Engineering, University of Hull, Hull HU6 7RX
Kyiv International University of Civil Aviation, 1, Ave. Cosmonaut
Komarov, Kiev, Ukraine 252058
Kyiv International University of Civil Aviation, 1, Ave. Cosmonaut
Komarov, Kiev, Ukraine 252058

Vadim Tokarev

1. INTRODUCTION

Ground operations at airports can make them noisy neighbours and lead to complaints from residents at substantial distances from the airport boundary. Although there are empirical schemes for predicting noise from engine testing [1,2], there has not been any systematic investigation of the extent to which noise levels can be predicted by available analytical models for outdoor sound propagation. In this paper, measurements of aircraft engine run-up noise out to distances of 3 km in the vicinity of airports are reported and analyzed. These data include the effects of source directionality, wavefront spreading, air absorption, interference between direct and ground-reflected waves, and diffraction. A particularly interesting feature in the data is the variation of attenuation rate with direction from the source. The data are compared with predictions for propagation from monopole and dipole sources near to impedance ground and for a monopole over discontinuous impedance ground. In the next part of the paper, the relevant ground effect models are outlined. The data and comparisons with predictions are detailed in the following section. Finally some conclusions are drawn.

2. GROUND EFFECT MODELS

In general, sound levels due to an aircraft engine, L , at an observer near to the ground may be calculated from a reference source level, L_{R0} , defined at reference point (R_0), corrected for power setting, directivity and for propagation effects. Hence

$$L = L_{R0} - \Delta L_M - \Delta L_\theta - \Delta L_{DIV} - \Delta L_{ABS} - \Delta L_{INT} - \Delta L_{DIF} \quad (1)$$

where ΔL_M is the correction for the power setting (engine mode); ΔL_θ is the correction for directivity; ΔL_{DIV} corrects for wave-front spreading; ΔL_{ABS} represents sound air absorption; ΔL_{INT} is the correction for sound wave interference (sometimes called ground effect) and ΔL_{DIF} allows for sound wave diffraction. In this paper, we are concerned particularly with ΔL_{INT} .

The total sound pressure at a point near the ground at height h_n has two main contributions: the first represents the direct sound from the source Φ (*direct wave*) and the second represents a contribution from an imaginary source beneath the surface, Φ_r (*reflected wave*), see fig. 3.1:

$$\Delta L_{INT} = 10 \lg \{ \Phi / \Phi_r \} \quad (2)$$

For a point source, the direct wave potential Φ , in spherical co-ordinates is defined by:

$$\Phi = \frac{\exp(ikR_1)}{R_1} \quad (3)$$

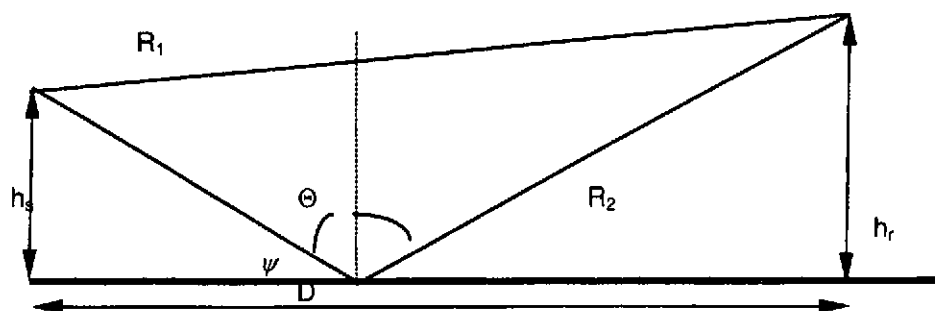


Figure 3.1 - Geometry of source and receiver

At an absorbing surface, the amplitude of the reflected wave is less than at a hard surface and there is a change in phase because of the time delay introduced during interaction with the surface. Both phenomena may be described by use of the complex surface impedance Z . The specific acoustic surface impedance is defined as the complex ratio of the effective sound pressure at a point of an acoustic medium to the effective particle velocity normal to the surface at the point. To characterize a ground surface it is usual to state the surface impedance normalized to the impedance of the air, $Z = Z_s / \rho c$, ρ - air density, c - speed of sound in an air. The admittance β is the inverse value of the impedance.

A convenient form for computation of the total field due a point source above an impedance ground [3], sometimes known as the Weyl-van der Pol solution, is

$$\Phi_t = \frac{\exp(ikR_1)}{R_1} + \{Q(\theta) + [1 - Q(\theta)]F(p_e)\} \frac{\exp(ikR_2)}{R_2} \quad (4)$$

where Q is sound-wave reflection coefficient from the surface, and $F(p_e)$ is the *boundary loss factor* and is a function of the «numerical distance» p_e . The boundary loss factor is the result of the interaction between the curved wave front and the flat reflecting surface.

$$F(p_e) = 1 + ip_e^{1/2} \exp(-p_e) \operatorname{erfc}(-ip_e); \quad p_e = (ikR_2/2)^{1/2} [\beta + \cos\theta]. \quad (5)$$

$$Q_p = \frac{Z \sin(\psi) - [1 - (k/k_2)^2 \cos^2(\psi)]^{1/2}}{Z \sin(\psi) + [1 - (k/k_2)^2 \cos^2(\psi)]^{1/2}}, \quad (6)$$

where ψ is the grazing angle (fig. 3.1); k , k_2 are the wave numbers for air and the reflecting medium.

Computation of the interference effect can be performed in a form of transmission loss:

$$TL = 10 \lg \left(\frac{p_t p_t^*}{p_d p_d^*} \right), \quad (7)$$

or by the formula [4]:

$$\Delta L_{INT} = 10 \lg(1 + S^2 |Q|^2 + 2S|Q|^* [\sin(\alpha^* dR/\lambda) / (\alpha^* dR/\lambda)] \cos[\alpha^* dR/\lambda + \delta]), \quad (3.11)$$

where $S = R_1/R_2$, $dR = (R_2 - R_1)$, $\alpha = \pi(df/f_i)$, df - width of frequency band, f_i - central frequency of the band, λ - wave length, $\beta = 2\pi[1 + (df/f_i)^2/4]^{1/2}$, for 1/3-octave bands $\alpha = 0,725$, $\beta = 6,325$.

De Jong [5] considered Pierce's formulation of sound diffraction from a wedge [6] with different surface acoustic impedances at either side. He then allowed the wedge to fold and derived his expressions for the propagation of sound from a point source over an impedance discontinuity. De Jong's expression can be re-written as;

$$P_t = \frac{e^{ikR_1}}{R_1} \left\{ 1 + (Q_b - Q_a) \frac{e^{-i\pi/4}}{\sqrt{\pi}} \cdot \frac{R_1}{R_d} F\left(\sqrt{k(R_d - R_1)}\right) \right\} + \frac{e^{ikR_2}}{R_2} \left\{ Q_{a,b} \pm (Q_b - Q_a) \frac{e^{-i\pi/4}}{\sqrt{\pi}} \cdot \frac{R_2}{R_d} F\left(\sqrt{k(R_d - R_2)}\right) \right\} \quad (8)$$

where R_1 and R_2 are the direct and image ray paths from the source to the receiver respectively, R_d is the source-discontinuity-receiver path. Subscripts a and b refer to the two impedance surfaces and $Q_{a,b}$ is the appropriate spherical reflection coefficient with $Q_{a,b}$ being equal to Q_a together with the +ve sign in the expression if the point of specular reflection falls in region b , and equal to Q_b together with the -ve sign, if the point of specular reflection falls in region a . The wave number is denoted by k and $F(x)$ is the Fresnel integral function. It is defined by

$$F(x) = \int_x^\infty e^{it^2} dt \quad (9)$$

The sound field due to a vertical dipole near an impedance plane can be approximated by [7]

$$p_v = \frac{S_1 \cos \gamma_l}{4\pi} \left\{ \cos \phi_s \left[\frac{1 - ikR_1}{R_1^2} \right] e^{ikR_1} + R_p \cos \theta_s \left[\frac{1 - ikR_2}{R_2^2} \right] e^{ikR_2} + \cos \mu_p (1 - R_p) F(w) \left[\frac{1 - ikR_2}{R_2^2} \right] e^{ikR_2} \right\}, \quad (10)$$

where $\sin \mu_p = \sqrt{1 - \beta^2}$, R_p and w are equivalent to Q_p and p_e used earlier.

This asymptotic solution is composed of three terms, a direct wave, a reflected wave and a ground wave term.

3. ANALYSIS OF DATA

Figure 1 shows the spectra and directivity from a low bypass engine (a D30-KP installed on an Ill'ushin-86 aircraft). Clearly the directivity of the radiation is important both in terms of intensity and spectrum.

The data on levels at various ranges were obtained over several days during the summer under fairly calm weather conditions (wind speed < 5 m/sec, temperature between 20°C and 25°C). The measurements were not intended for the study of particular propagation effects but for assessment of overall sound level ($OASPL$ and L_A) relationships. In spite of this, the data provide an indication of the form and extent of ground attenuation of noise propagated in various directions from aircraft engine run-ups. For the purposes of this analysis, all the data have been expressed as horizontal level differences with respect to a reference level at 100m.

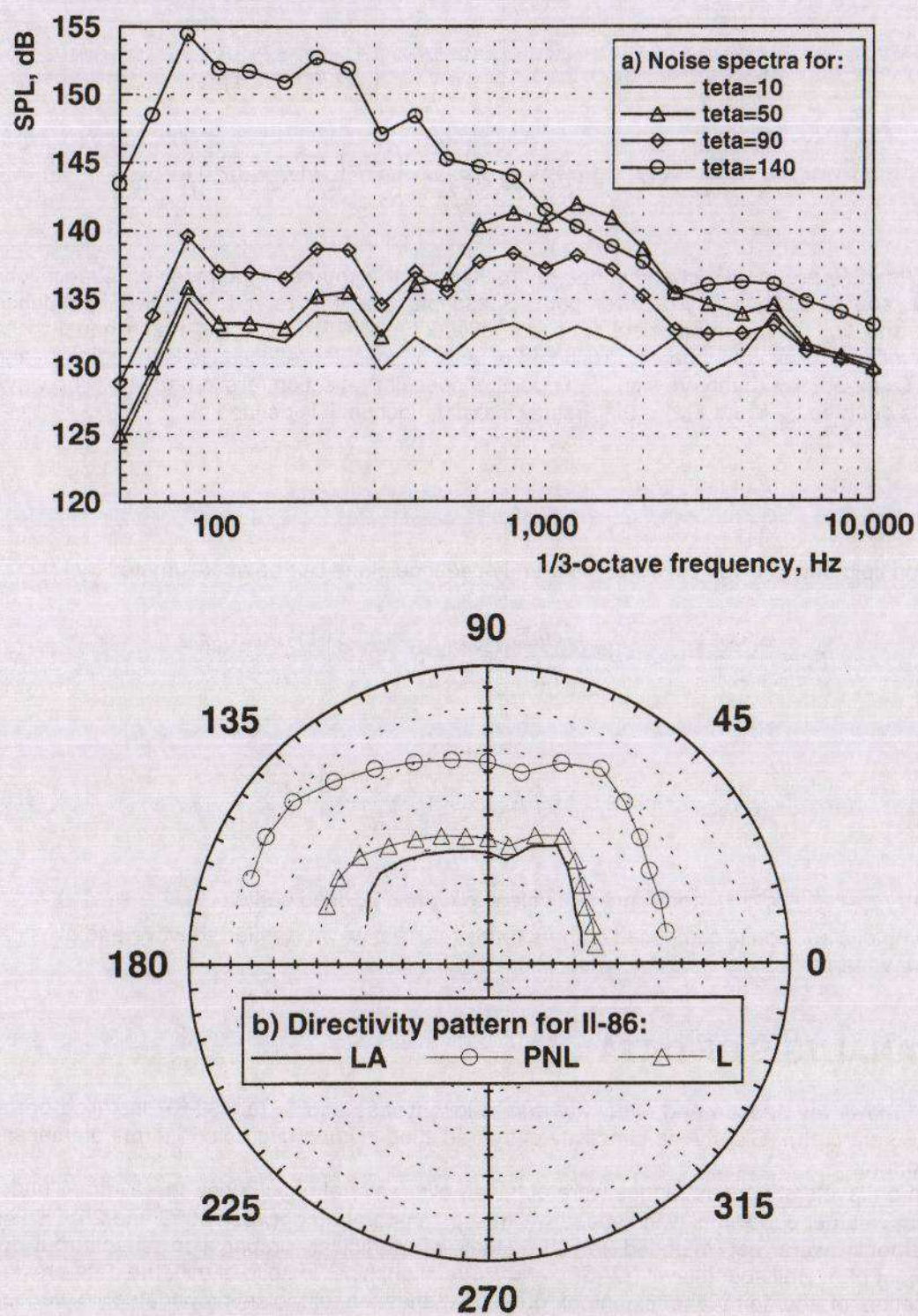


Figure 1 – Noise spectra and directivity patterns of sound generation by D30-KP engine at maximum power (reference distance = 1 m)

The data presented in figure 2 were obtained in the direction of maximum jet noise generation ($\theta \cong 140^\circ$) from a D30-KP engine (on an Il'ushin aircraft). The data presented in Figure 3 are for

propagation in the direction of maximum propeller noise from an Al-24 turbo-prop engine (An-24 aircraft). These data are compared with the calculated level differences due to a monopole source including the effects of sound wave spreading (divergence) and air absorption (Div+Abs). Level differences predicted for propagation over three kinds of surface covering (concrete, grass and soil) are presented also.

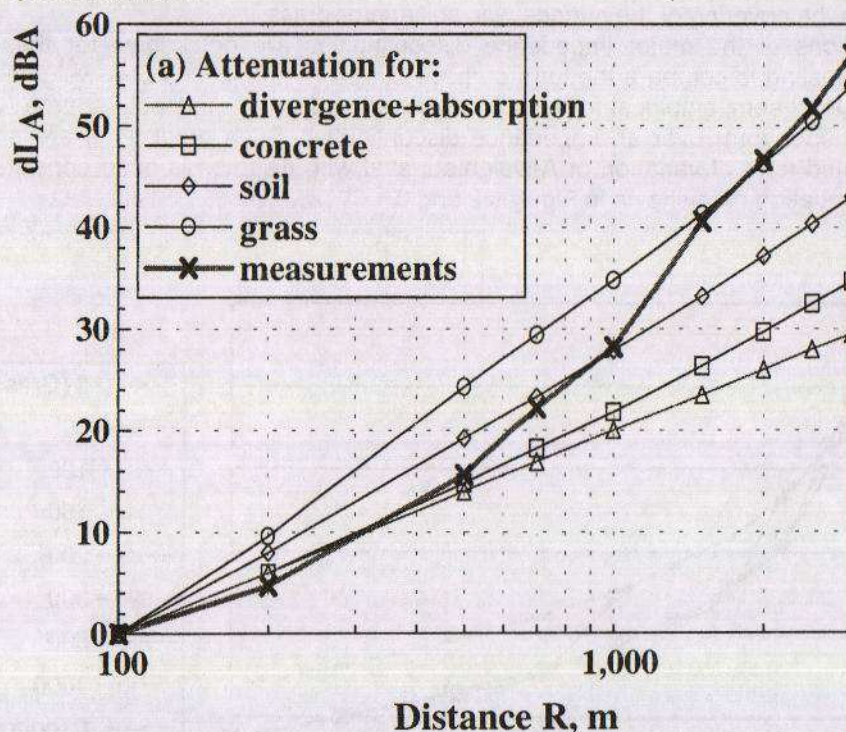


Figure 2 - Sound level difference dB re 100 m for noise propagating from Il-86 aircraft's engine in the direction of maximum jet noise generation

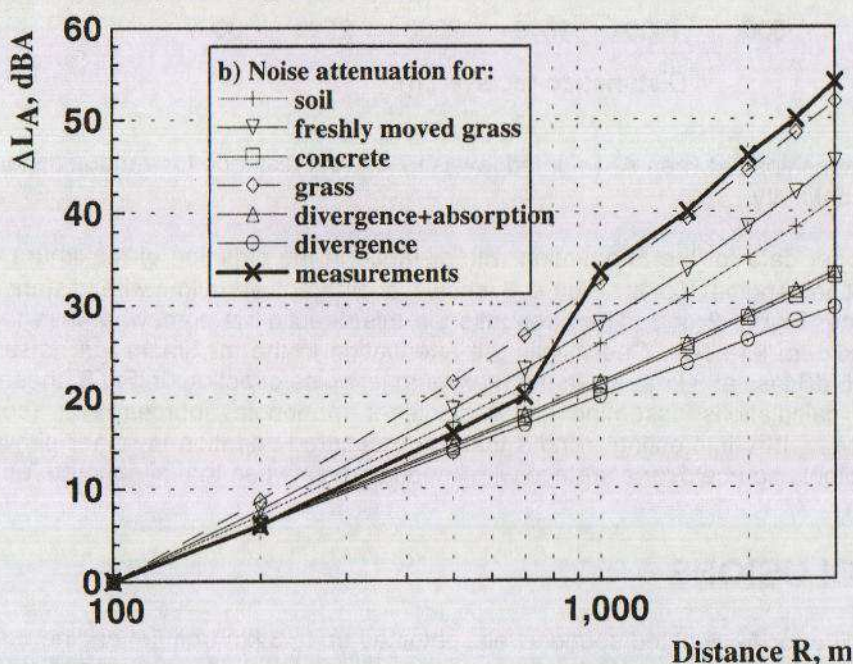


Figure 3 - A-weighted Sound level difference dB re 100m for noise propagating from Al-24 turbo-prop engine (An-24 aircraft) in the direction of maximum propeller noise generation

Near to the source (< 500 or 700 m), it is clear that both sets of data conform to the predicted propagation over a hard surface (the «Concrete» line). Further away (>500 or 700 m), the data lie nearer near to «Soil» predictions or between the «Soil» and «Grass» predictions. This is consistent with the fact that the run-ups took place over the concrete surface of an apron whereas at larger distances the covering of the surface was soil and/or grass.

The precise locations of the major impedance discontinuities are not known for these data. However, it is interesting to compare the form of these data with predictions of A-weighted levels based on the De Jong semi-empirical formula for propagation from a monopole source (with the Il'ushin-86 engine spectrum) over an impedance discontinuity. Such predictions are shown in Fig.4. The predicted form of variation of A-weighted level with distance is quite consistent with the measured attenuation data shown in Figures 2 and 3.

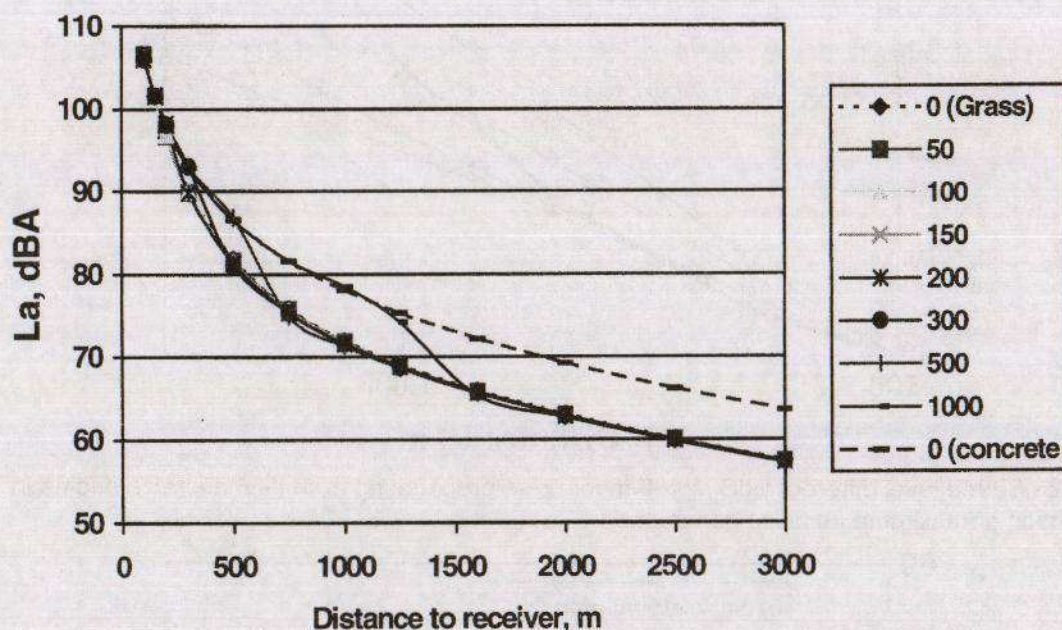


Figure 4 –Relationships between A-weighted levels L_A dB and distance for various distances to the point of discontinuity

Finally we consider data for the attenuation with distance in the direction of maximum fan noise from an aircraft jet engine (60°). Figure 5 shows a different variation with distance to that displayed in either Figure 2 or 3. The attenuation in this direction is somewhat less than in the direction of maximum jet noise. Specifically the attenuation in the maximum fan noise direction appears to be 15 dB less at 3 km than in the maximum jet noise direction. In Fig.5, these data are compared with calculations assuming either dipole or monopole sources over (continuous) impedance planes. It is interesting to note that the measured variation is rather similar to that predicted for a dipole source over a surface with impedance between that of concrete and grass.

4. CONCLUSIONS

An analysis of data for A-weighted sound levels, obtained up to 3 km from jet engine run-up tests around an airport, reveals a considerable variation in attenuation rate with direction. The measured attenuation in the maximum jet and fan noise directions have been compared with predictions. It is found that the form of the measured attenuation with distance in the maximum jet

noise direction is similar to that predicted for a monopole source (with the relevant spectrum) over an impedance discontinuity. On the other hand, the form of the measured attenuation with distance in the maximum fan noise direction is consistent with the predicted attenuation from a dipole over a (continuous) impedance plane. The measured attenuation from a propeller engine run-up in the direction of maximum propeller noise is similar to that predicted for a point source radiating over an impedance discontinuity. Although the primary source type in propeller and fan noise is dipole, the primary sources in jet noise are quadrupole in nature. A model of ground effect for a quadrupole source over an impedance plane is available already [8]. However, further work would be needed to develop a more accurate model for such complex sources near to discontinuous impedance boundaries. Nevertheless, this preliminary analysis has indicated the possibility that the character of the source, its directivity in particular, might play as large a part as the nature of the ground surface in determining noise levels around engine testing facilities.

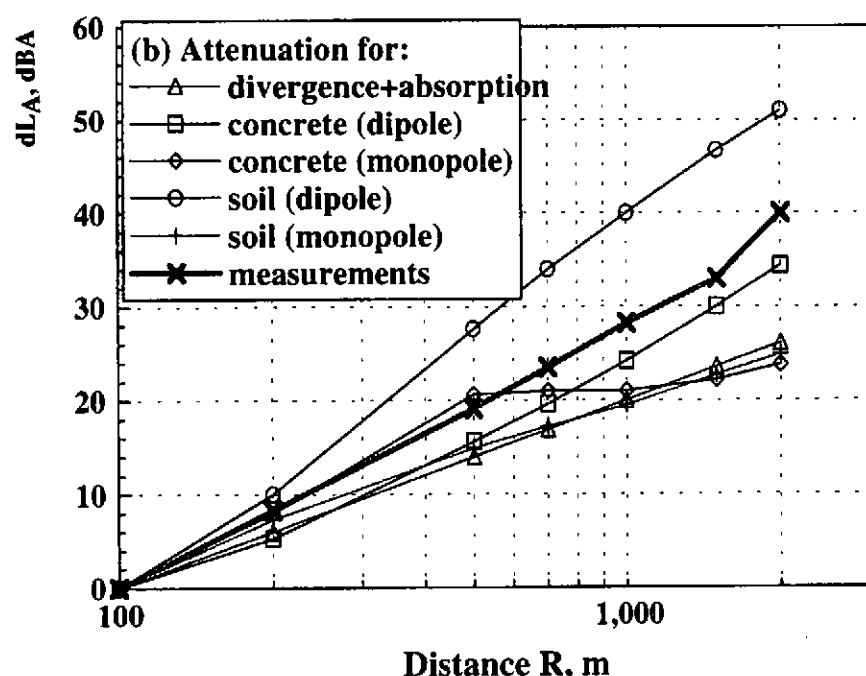


Figure 5 - Sound level difference dB re 100 m for noise propagating from an II-86 aircraft engine in the direction of maximum fan noise generation

ACKNOWLEDGEMENT

This work was supported in part by NATO Grant No. CLG 974767

REFERENCES

- 1 ISO 9613/2 1996 «Acoustics - Attenuation of sound during propagation outdoors»
- 2 Prediction Method for Lateral Attenuation of Airplane Noise During Take-off and Landing, SAE, AIR 1751, 1981.
- 3 Chien C.F., Soroka W.W. Sound propagation along an impedance plane, J. Sound Vib. **43**, No 1, 1975. - p. 9 - 20. and A note on the calculation of sound propagation along an impedance boundary, J. Sound Vib. **69**, No 1, 1980.
- 4 Chessel C.I. Propagation of noise along a finite impedance boundary, J. Acoust. Soc. Am. **62**, 1977. - p. 825-834.
- 5 B.A. De Jong, A. Moerkerken and J.D. van Der Toorn, "Propagation of sound over grassland and over an earth barrier", J. Sound Vib., **86**, 23-46, (1983)

Proceedings of the Institute of Acoustics

6 A.D. Pierce, "Diffraction of sound around corners and over wide barriers", J. Acoust. Soc. Am., 55(5), 941-955, (1974)

7 K. M. Li, S. Taherzadeh and K. Attenborough, "Sound propagation from a dipole source near an impedance plane", J. Acoust. Soc. Am. 101 (6) 3343 - 3352 (1997)

8 K. M.Li and S. Taherzadeh, The sound field of an arbitrarily-orientated quadrupole near ground surfaces, J. Sound Vib. 1998